Statistical analysis on random quantum circuit sampling by Sycamore and Zuchongzhi quantum processors

Sangchul Oh and Sabre Kais

Statistical Analysis on Random Quantum Circuit Sampling by Sycamore and Zuchongzhi Quantum Processors

Sangchul Oh[*] and Sabre Kais[†]

Department of Chemistry, Department of Physics and Astronomy,
and Purdue Quantum Science and Engineering Institute, Purdue University, West Lafayette, IN, USA
(Dated: September 16, 2022)

Random quantum circuit sampling, a task to sample bit-strings from a random quantum circuit, is considered one of suitable benchmark tasks to demonstrate the outperformance of quantum computers even with noisy qubits. Recently, random quantum circuit sampling was performed on the Sycamore quantum processor with 53 qubits [Nature **574**, 505 (2019)] and on the Zuchongzhi quantum processor with 56 qubits [Phys. Rev. Lett. **127**, 180501 (2021)]. Here, we analyze and compare statistical properties of the outputs of random quantum circuit sampling by the Sycamore and Zuchongzhi processors. Using the Marchenko-Pastur law of random matrices of bit-strings and the Wasssertein distances between bit-strings, we find that statistical properties of Sycamore bit-strings are quite different from those of Zuchongzhi bit-strings while both processors score similar values of linear cross-entropy fidelity for random circuit sampling. Some bit-strings sampled by the Zuchongzhi processor pass the NIST random number tests while both Sycamore and Zuchongzhi processors show similar patterns in heatmaps of bit-strings. Zuchongzhi bit-strings are much closer to classical uniform random bits than those of Sycamore. It is shown that the statistical properties of bit-strings of both random quantum circuits change little as the depth of random quantum circuits increases. Our findings raise a question about computational reliability of noisy quantum processors because two quantum processors with similar noise levels and similar qubit structures produced statistically different outputs for the same random quantum circuit sampling.

I. INTRODUCTION

A quantum computer is believed to simulate quantum systems much better [1] and to solve some computational tasks exponentially faster [2, 3] than a classical computer. A demonstration of the outperformance of a quantum computer, called quantum supremacy [4] or quantum advantage, is considered one of the important milestones in developing practical quantum computers. Random quantum sampling [5] is regarded as a good candidate for demonstrating quantum advantage with noisy intermediate-scale quantum (NISQ) computers available these days. Recently, quantum advantage has been claimed for random quantum circuit sampling on the Sycamore quantum processor with 53 superconducting qubits [6] and the Zuchongzhi quantum processor with 56 superconducting qubits [7], and for Boson sampling with optical qubits [5, 8, 9].

Quantum advantages of the Sycamore and Zuchongzhi quantum processors over classical computers for random quantum circuit sampling were verified using the linear cross-entropy benchmarking (XEB) fidelity, whose values were estimated slightly larger than zero [6, 7]. Both quantum processors are made of two-dimensional arrays of superconducting transmon qubits, have similar error rates, executed the same random quantum circuit, and scored similar XEB values. So, one may speculate that the output bit-strings generated by the two noisy quantum processors would be statistically close as two classical computers with the same architecture usually produce the same results for the same inputs or statistically close results for stochastic calculations. However, it is unknown whether two noisy quantum processors with similar values of the XEB fidelity generate statistically similar bit-strings or not. In this paper, we analyze the statistical closeness of the outputs of the two noisy quantum processors using the NIST random number tests [10], the Marchenko-Pastur distribution of eigenvalues of random matrices of bit-strings [11], and the Wasserstein distance between samples [12]. We show that Sycamore's random bit-strings are farther away from classical uniform random bit-strings than Zuchongzhi's outputs, that is, the two outputs of bit-strings are noticeably different.

II. RANDOM QUANTUM CIRCUIT SAMPLING

Let us first summarize random quantum circuit sampling implemented on the Sycamore and Zuchongzhi quantum processors [6, 7]. The task of random quantum circuit sampling is to sample bit-strings $x = a_1 \cdots a_n \in \{0, 1\}^n$ by applying a random quantum circuit U on the initial state $|0\rangle$ of n qubits followed by the measurement. Both Sycamore and Zuchongzhi quantum processors executed the same random quantum circuit U composed of m cycles as follows. A quantum circuit U_k at the k-th cycle consists of single-qubit gates R selected randomly from the set $\{\sqrt{X}, \sqrt{Y}, \sqrt{W}\}$ on all qubits and deterministic two-qubit gates on the pair of qubits selected in the sequence of the coupler activation patterns of 2-dimensional superconducting qubits. After m cycles, a final single-qubit gate R is applied before the measure-

---

[*] oh.sangchul@gmail.com
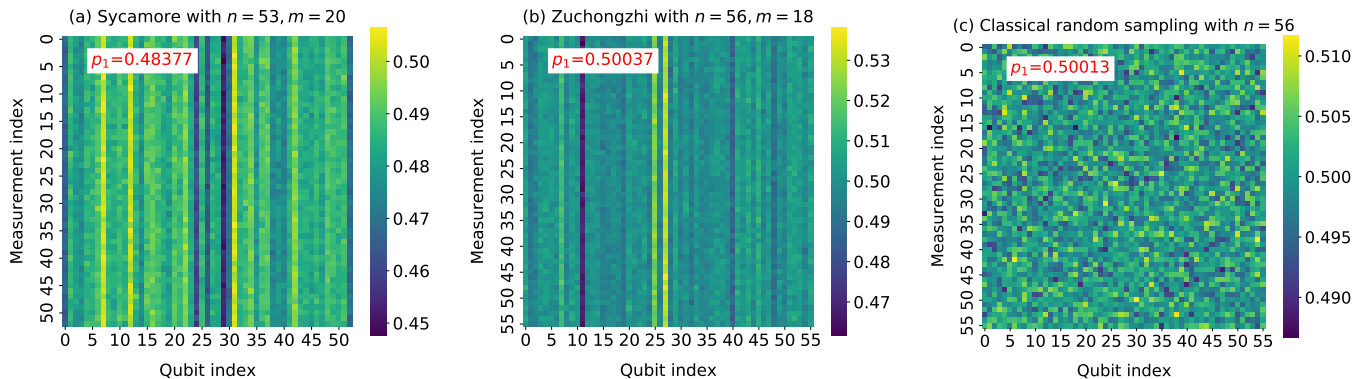[†] Corresponding author: kais@purdue.edu

FIG. 1. Heatmaps of bit-strings of random quantum circuit sampling are plotted for (a) the Sycamore quantum processor with $n = 53$ qubits, $m = 20$ cycles, and sample numbers $M = 10^6$, (b) the Zuchongzhi quantum processor with $n = 56$ qubits, $m = 20$ cycles, and $M = 10^6$ samples, and (c) classical uniform random sampling with $n = 56$ and $M = 10^6$. The average of finding bit 1 of bit-strings is denoted by p_1. Random quantum samples, (a) and (b), show the stripe patterns at specific qubit indices while (b) and (c) pass the NIST random number tests.

ment, so the whole random quantum circuit with cycle m is given by $U = RU_mU_{m-1}\cdots U_1$. The output of the random quantum circuit is a bit-string x that is sampled from the probability $p(x) = |\langle x|\, U\, |0\rangle|^2$. By implementing the same random quantum circuit M times, a collection of M random bit-strings $\mathcal{D} = \{x_1, \ldots, x_M\}$, i.e., an $M \times n$ binary bit array, is obtained.

To verify that a noisy quantum processor is performing random quantum circuit sampling well [6, 7], the linear cross-entropy benchmarking (XEB) fidelity F_{XEB} is introduced

$$F_{\mathrm{XEB}} = 2^n \cdot \frac{1}{M} \sum_{x \in \mathcal{D}} p(x) - 1\,, \qquad (1)$$

where the ideal probability $p(x) = |\langle x|\, U\, |0\rangle|^2$ of finding a bit-string x is computed on a classical computer using Schrödinger or Feynman simulators and the bit-strings $\mathcal{D} = \{x_1, \ldots, x_M\}$ are generated by a quantum processor. It is known that $F_{\mathrm{XEB}} = 1$ if a quantum processor implements a random quantum circuit without errors, and $F_{\mathrm{XEB}} = 0$ if bit-strings are sampled from a classical uniform distribution. The estimated XEB fidelity of Sycamore is $F_{\mathrm{XEB}} = (2.24 \pm 0.021) \times 10^{-3}$ for 53 qubits, 20 cycles, and $M = 30 \times 10^6$ samples over 10 circuit instances [6]. For the Zuchongzhi quantum processor [7], the estimated XEB fidelity is $F_{\mathrm{XEB}} = (6.62 \pm 0.72) \times 10^{-4}$ for 56 qubits, 20 cycles, and $M = 1.9 \times 10^7$ samples.

While the XEB fidelity could serve as a benchmark for quantum advantage of random quantum circuit sampling, it has some limitations. The XEB fidelity stems from the Kullback-Leibler divergence or the cross entropy of an empirical probability distribution $\tilde{p}(x)$ of the data $\mathcal{D}$ from the ideal probability distribution $p(x)$ [13]. As the number of qubits increases, it is very difficult to calculate both probability distributions. The number of samples required to construct the empirical probability $\tilde{p}(x)$ increases exponentially because the range of $x \in [0, 2^n - 1]$ does as well. While the XEB fidelity needs only an

ideal probability $p(x)$ but not $\tilde{p}(x)$, it is still not scalable because in quantum advantage regime a supercomputer cannot calculate the ideal probability $p(x)$ in Eq. (1) and no other NISQ processors could do so. Recently, the limitations of the XEB fidelity as a benchmark for quantum advantage have been pointed out by Gao *et. al.* [14]. More importantly, the XEB fidelity could not give any clue about statistical properties of bit-strings of random quantum circuit sampling implemented on NISQ processors.

III. COMPARISON OF RANDOM QUANTUM CIRCUIT SAMPLING OF SYCAMORE AND ZUCHONGZHI

A simple way of comparing the performance of two quantum processors is to compare directly their outputs of a task, here random quantum circuit sampling. Both Sycamore and Zuchongzhi quantum processors are composed of transmon qubits and have the similar noise levels. The averages of single-qubit gate errors, two-qubit gates errors, and the readout error of Sycamore is about 0.15%, 0.36%, and 3.1%, respectively [6]. The average errors of Zuchongzhi are about 0.14% for single-qubit gates, 0.59% for two-qubit gates, and 4.52% for readout, respectively [7]. Both processors implemented the same random quantum circuit as described before and obtained similar values of XEB fidelity. So, one may expect that their outputs would be statistically close to each other. However, that is not the case. Both Sycamore and Zuchongzhi showed similar exponential decays of the XEB fidelity F_{XEB} as a function of qubit number n or cycle m [6, 7].

We first examine whether the output bit-strings of random quantum circuit sampling are random or not while random circuit sampling is not intended to generate random numbers. There are simple quantum mechanical ways of generating random numbers [15]. Random num-

bers have many practical applications in Monte-Carlo simulation, statistics, cryptography, etc. Given a random quantum circuit U, the probability $p(x) = |\langle x| U |0\rangle|^2$ of finding bit-string x is not uniform due to the entanglement and interference, so some bit-strings are more likely to be sampled than others. However, there is no physical ground that the output of bit-strings $\mathcal{D} = \{x_1, x_2, \ldots, x_M\}$ would contain more bit 1 than 0 or vice versa. Bits 0 and 1 are equally probable if there is no error. To see this, the output of bit-strings $\mathcal{D}$ is sliced into the collection of $n \times n$ binary arrays, with which the heatmaps are plotted as shown in Fig. 1. Fig. 1 (a) depicts the heat map of Sycamore's bit-strings for $n = 53$ qubits, $m = 20$ cycles, and $M = 3 \times 10^6$ samples [16]. Fig. 1 (b) displays the heatmap of Zuchongzhi's bit-strings for $n = 56$ qubits, $m = 18$ cycles, and $M = 3 \times 10^6$ samples. Fig. 1 (c) shows the heatmap of uniform random bits sampled from a classical computer for $n = 56$ and $M = 3 \times 10^6$. As depicted in Fig. 1, the heatmaps of random quantum circuit sampling on Sycamore and Zuchongzhi quantum processors show bright and dark stripes at some qubit indices while the classical uniform random sampling does not. One may suspect that stripe patterns could be caused by readout errors. However, for both Sycamore and Zuchongzhi data sets, the locations of bright or dark stripes in the heatmaps do not coincide with the indices of qubits with high readout errors.

We count the number of bit 1 contained in the output bit-strings $\mathcal{D} = \{x_1, \cdots, x_M\}$. The average of finding bit 1 is denoted by p_1. Most Zuchongzhi outputs show p_1 is greater than $1/2$, as shown in Supplementary Material [17], while all Sycamore outputs have p_1 less than $1/2$ [18]. As depicted in Fig. 1, Zuchongzhi's bit-strings with $n = 56$ qubits, $m = 18$ cycles have $p_1 = 0.50094$ while Sycamore's bit-strings for $n = 53$ qubits and $m = 20$ cycles have $p_1 = 0.48383$. Note that the readout errors of Sycamore and Zuchongzhi are reported to be 3.1% and 4.52%, respectively. It is unclear why Sycamore and Zuchongzhi are quite different in the probability p_1 of finding bit 1 in random quantum circuit sampling.

To see the randomness of bit-strings, we perform the NIST random number tests [10] for Zuchongzhi's outputs. We find that some Zuchongzhi data sets pass the NIST random number tests while all Sycamore data sets do not [17, 18]. Note that the probability p_1 of finding bit 1 is related to the frequency test of the NIST random number tests. It is interesting to see that some Zuchongzhi data sets pass the NIST random number tests while all random quantum circuit sampling data of Sycamore and Zuchongzhi show the stripe patterns unlike the classical uniform random samples, as shown in Fig. 1. This implies random quantum circuit sampling may be used to generate quantum random numbers [15, 19].

If bit-strings are sampled from the classical uniform random distribution $p_{\text{cl}}(x) = 1/2^n$. Using the Marchenko-Pastur distribution [11] and the Wasserstein distances [12, 20], we examine how the random bit-string

outputs of Sycamore and Zuchongzhi are far away from classical uniform random samples as a function of qubit number n and cycle m.

The signal out of randomness can be captured by the outliers of the Marchenko-Pastur distribution of random matrices. This method has been applied to the covariance matrices in finance [21, 22] in predicting ligand affinity [23], and in denoising MRI [24] and single-cell data [25]. We use the Marchenko-Pastur distribution of eigenvalues of random bit-strings to measure the distance among Sycamore's outputs, Zuchongzhi's outputs, and classical uniform random samples. The data $\mathcal{D} = \{x_1, x_2, \ldots, x_M\}$, an binary $M \times n$ array, is sliced into the collection of $k \times n$ random matrices X. All entries of X are assumed to be independent and identically binary random variable $\{0, 1\}$ with the mean $\mu_X = 1/2$ and the variance $\sigma_X^2 = 1/4$. We calculate the empirical distribution of eigenvalues of $n \times n$ matrix $\frac{1}{k} X^t \cdot X$, as shown in Fig. 2. The empirical eigenvalue distribution is composed of the two parts: the bulk corresponding to the noise or random and the outliers representing the signal. To understand this, let us consider the transformed random matrix $Y = 2X - J$ with J of all entries 1. The matrix $\frac{1}{k} X^t \cdot X$ is written as

$$\frac{1}{k} X^t \cdot X = \frac{1}{4k} \left(Y^t \cdot Y + X^t \cdot J + X^t \cdot Z + J^t \cdot J \right). \quad (2)$$

The matrix Y has the mean $\mu_Y = 0$ and the variance $\sigma_Y^2 = 1$. The eigenvalue distribution of the first term in Eq. (2), $\frac{1}{k} Y^t \cdot Y$, follows the Marchenko-Pastur distribution [11]

$$\rho(\lambda) = \frac{1}{2\pi\sigma^2\gamma} \frac{\sqrt{(\lambda_+ - \lambda)(\lambda - \lambda_-)}}{\lambda}, \quad (3)$$

where $\gamma = n/k$ is the rectangular ratio and $\lambda_\pm = \sigma^2(1 \pm \sqrt{\gamma})^2$ are the upper and lower bounds. Here we take $k = 2n$, i.e., $\gamma = 1/2$. The upper limit is given by $\lambda_+ = 1 + \sqrt{1/2}$. By considering the scaling factor $1/4$, the upper limit of $(1/4k) \cdot Y^t \cdot Y$ is given by $(1 + \sqrt{1/2})/4 \approx 0.7285$. The last term of Eq. (2), $(1/4k)J^t \cdot J$ has the two eigenvalues, 0 and $n/4$. So the outliers are located around $n/4$.

Figs. 2 (a) and (b) plot the empirical distributions of eigenvalues of $\frac{1}{k} X^t \cdot X$ made of Sycamore bit-strings with $n = 51$, $m = 14$, and $M = 10^6$ (red color), Zuchongzhi bit-strings with $n = 51$, $m = 10$ and $M = 10^6$ (blue color), and classical uniform random bits with $M = 10^6$ (green color). As shown in Fig. 2 (b), the outlier peak of Sycamore is located at the left of $n/4$ while the outlier peaks of Zuchongzhi and classical random sampling are located at right of $n/4$. Surprisingly, Zuchongzhi's bit-strings are much closer to the classical random bit strings than Sycamore's ones while Sycamore and Zuchongzhi have similar values of the XEB fidelity. As shown in Fig. 2 (c), both Sycamore and Zuchongzhi quantum processors show similar exponential decreases of the XEB fidelity of random circuit sampling as the number of qubits
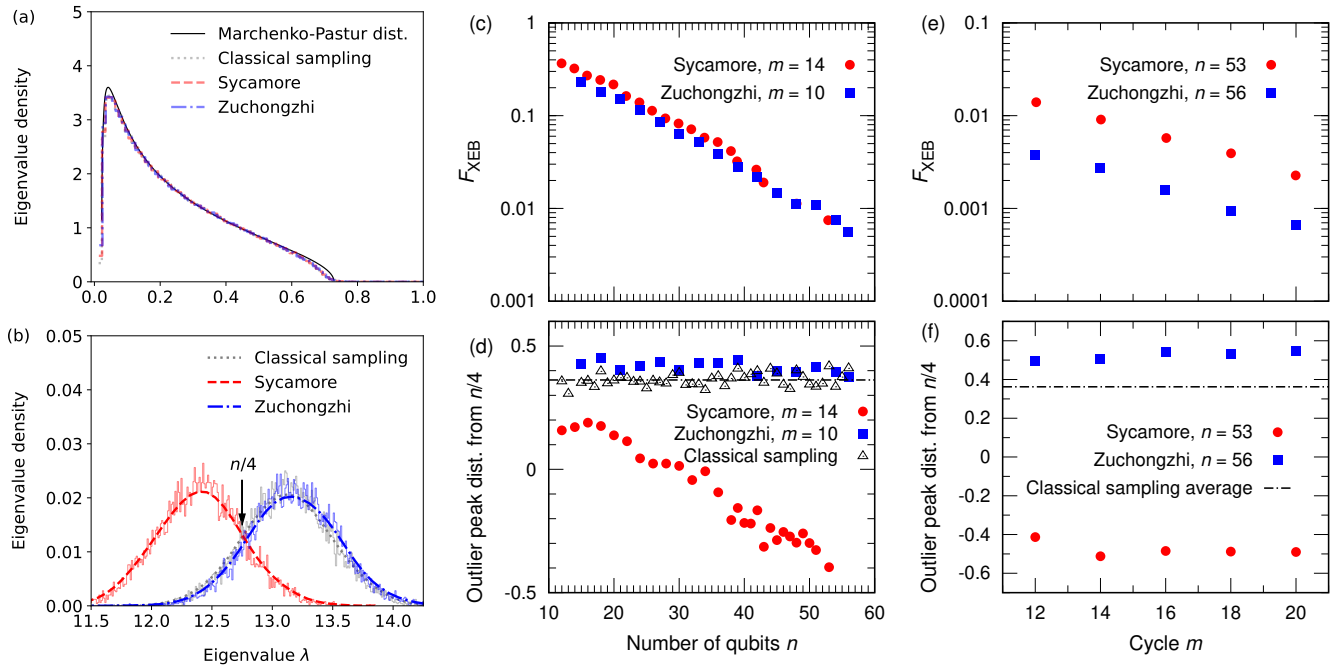
FIG. 2. (a) For $n = 51$ qubits, the bulk distributions of eigenvalues of random matrices $\frac{1}{k}X^t X$ of of classical random bit-strings (gray dotted line), the Sycamore bit-strings (red dashed line), and the Zuchongzhi bit-strings (blue dashed-dotted line) obey the Marchenko-Pastur law, Eq. (3). (b) The outliers of the Marchenko-Pastur distribution of eigenvalues of classical random bit-strings (gray dotted line), Sycamore's bit-strings (red dashed line), and Zuchongzhi's bit-strings (blue dash-dotted line) are distributed around $n/4$. (c) The plots of the XEB fidelity F_{XEB} for Sycamore (red solid circle) and Zuchongzhi (blue solid square) random circuit sampling as a function of the number of qubits n are shown together for comparison. The Sycamore and Zuchongzhi XEB fidelity data are taken through digitizing Figs. 4 (a) of Arute *et al.* [6] and Wu *et al.* [7], respectively. (d) The outlier peaks of the Marchenko-Pastur distribution from $n/4$ are plotted as a function of the qubit number n for Sycamore, Zuchongzhi, and classical random sampling (black triangle). (e) The XEB fidelity is plotted as a function of cycle m for Sycamore with $n = 53$ [6] and Zuchongzhi with $n = 56$ [7]. (f) The distances of the outlier peaks of the Marchenko-Pastur distributions from $n/4$ are plotted as a function of cycle m for the Sycamore processor with $n = 53$ and the Zuchongzhi processor with $n = 56$.

n increases. Fig. 2 (c) is plotted by digitizing the graph of Figs. 4 (a) of Ref. [6] and Ref. [7]. Fig. 2 (d) plots the distances of the outlier peaks of the Marchenko-Pastur distributions from $n/4$ as a function of qubit number n. The Sycamore processor becomes farther away from $n/4$ as n increases. On the other hands, Zuchongzhi's distance from $n/4$ changes a little. The outlier peak distances from $n/4$ show that the two processors generated statistically different bit-strings while both scored the same values of the XEB fidelity. Fig. 2 (e) shows the exponential decays of the XEB fidelity as a function of cycle m for the Sycamore processor with $n = 53$ qubits and the Zuchongzhi processor with $n = 56$ qubits. Fig. 2 (f) plots the outlier peak distances from $n/4$ as a function of cycle m for the both processors, which change little as cycle m increases. This is also in contrast with the exponential decay behavior of the XEB fidelity as a function of cycle m.

The statistical distances among Sycamore, Zuchongzhi, and classical random sampling, based on the Marchenko-Pastur distribution, can be further confirmed by calculating the Wasserstein distances. The 1-

Wasserstein distance between two probability distributions $p(x)$ and $q(x)$ [12] is defined by

$$W(P, Q) = \inf_{\pi \in \Pi(p,q)} \mathbb{E}_{(x,y) \sim \pi} \left[||x - y|| \right], \qquad (4)$$

where $\Pi(p, q)$ is the set of all joint distributions $\pi(x, y)$ whose marginal distributions are $p(x)$ and $p(y)$, respectively. Given two samples, $\{x_1, x_2, \ldots, x_M\}$ and $\{y_1, y_2, \ldots, y_M\}$, $W(p, q)$ can be calculated directly without calculating the empirical distributions $p(x)$ and $q(x)$ [20]. The Wasserstein distance is a true metric on a probability space, so the relative Wasserstein distances among Sycamore, Zuchongzhi, and classical random sampling give rise to the triangle inequality. Fig. 3 (a) plots the triangle relation among the three data sets for $n = 18, 24, 30, 36, 42, 45, 48, 51$. All Zuchongzhi data sets are closer to classical random sampling than Sycamore. This is consistent with the outlier peak distances from $n/4$ of the Marchenko-Pastur distributions as a function of qubit number n, as shown in Fig. 2 (d). Fig. 3 (b) plots the Wasserstein distance of Sycamore $n = 53$ and Zuchongzhi $n = 56$ from the classical random bit-strings
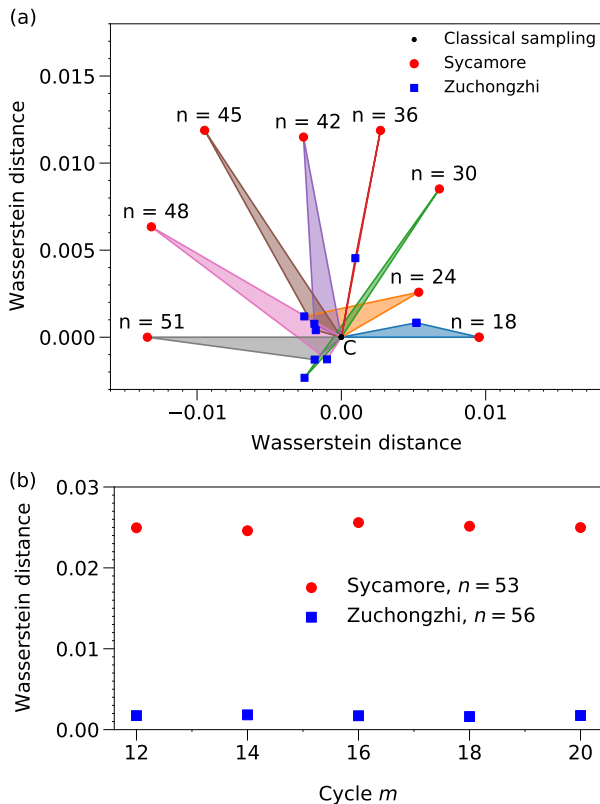
FIG. 3. (a) For qubits $n = 18, 24, 30, 36, 42, 45, 48, 51,$ the relative positions of Sycamore (red circle), Zuchongzhi (blue square), and classical random sampling (black circle at origin) form triangles whose edges are the Wasserstein distances. For clarity, triangles are rotated. (b) for Sycamore bit-strings with $n = 51$ and Zuchongzhi with $n = 56$, the Wasserstein distances from the classical random sampling are plotted as a function of cycle m.

as a function of cycle m. This result is consistent with the behavior of the relative distances of the outliers of the Marchenko-Paster distribution as a function of m, shown in Fig. 2 (e). Note that the Wasserstein distances between the bit-strings with different cycles of Sycamore (or Zuchongzhi) are less than the Wasserstein distance of them from the classical random sampling. It is found that the statistical properties of output bit-strings, here the position of the outlier peak of the Marchenko-Pastur distribution or the Wasserstein distance, depend only on the number of qubits n and the number of cycles m, but not on random seeds of random quantum circuits, i.e. the samples from different random circuits have similar behavior in our tests due to concentration properties. This is analogous to the fact that the Monte-Carlo integration depends on the number of throws, but not on a random seed of a random number generator.

IV. CONCLUSION

In this paper, we analyzed the statistical properties of random bit-strings sampled from Sycamore and Zuchongzhi quantum processors using the heatmaps, the NIST random number tests, the Marchenko-Pastur distribution, and the Wasserstein distances. Both Sycamore and Zuchongzhi exhibit stripe patterns in the heatmaps of random bit-strings. Some of Zuchongzhi's data pass the NIST random number tests. This may open up a possibility of the use of the random quantum circuit as a quantum random number generator. The Marchenko-Pastur distribution and the Wasserstein distances of random bit-strings shows that Zuchongzhi random quantum circuit sampling is statistically much closer to classical random sampling than Sycamore's, while both have similar error rates and similar values of the XEB fidelity. The distances of random bit-strings of Sycamore from the classical uniform sampling as a function of the number of qubits n is quite different from those of Zuchongzhi. The distances of Sycamore's and Zuchongzhi's bit-strings from the classical random bit-strings remain almost constant as the cycle number m increases. This is in contrast with the exponential decay of the XEB fidelity as a function of m.

The results found here raise a question about the computational reliability and verification of noisy quantum processors [26]. Two classical computers performing the same task will produce the same outputs (within statistical errors for stochastic calculation). One may expect that two NISQ processors with similar error rates would produce statistically close outputs. If two quantum gates are close to each other, the probability distributions of measurement outcomes for each quantum gate operation are close too [27]. If a random quantum circuit of the Sycamore quantum processor is close to that of the Zuchongzhi processor and noisy levels of both qubits are similar, then the difference in probabilities of output bit-strings of the two processors would be small. However, there is the noticeable difference in the statistical properties of bit-strings for random circuit sampling for the two processors. This means that either the two devices have very different noise models (despite having similar gate fidelities), or there may exist an unknown fact that caused this difference. In order to ensure the reliability of quantum computing with NISQ quantum processors, it is necessary to have good benchmark tools which can verify the output of quantum calculation on a classical computer, until fully error-corrected quantum computers are available.

[1] R. P. Feynman, International Journal of Theoretical Physics **21**, 467 (1982).

[2] P. W. Shor, SIAM Journal on Computing **26**, 1484 (1997).

[3] A. W. Harrow, A. Hassidim, and S. Lloyd, Phys. Rev. Lett. **103**, 150502 (2009).

[4] J. Preskill, Quantum computing and the entanglement frontier (2012), arXiv:1203.5813 [quant-ph].

[5] S. Aaronson and A. Arkhipov, Theory of Computing **9**, 143 (2013).

[6] F. Arute, K. Arya, R. Babbush, D. Bacon, J. C. Bardin, R. Barends, R. Biswas, S. Boixo, F. G. S. L. Brandao, D. A. Buell, B. Burkett, Y. Chen, Z. Chen, B. Chiaro, R. Collins, W. Courtney, A. Dunsworth, E. Farhi, B. Foxen, A. Fowler, C. Gidney, M. Giustina, R. Graff, K. Guerin, S. Habegger, M. P. Harrigan, M. J. Hartmann, A. Ho, M. Hoffmann, T. Huang, T. S. Humble, S. V. Isakov, E. Jeffrey, Z. Jiang, D. Kafri, K. Kechedzhi, J. Kelly, P. V. Klimov, S. Knysh, A. Korotkov, F. Kostritsa, D. Landhuis, M. Lindmark, E. Lucero, D. Lyakh, S. Mandrà, J. R. McClean, M. McEwen, A. Megrant, X. Mi, K. Michielsen, M. Mohseni, J. Mutus, O. Naaman, M. Neeley, C. Neill, M. Y. Niu, E. Ostby, A. Petukhov, J. C. Platt, C. Quintana, E. G. Rieffel, P. Roushan, N. C. Rubin, D. Sank, K. J. Satzinger, V. Smelyanskiy, K. J. Sung, M. D. Trevithick, A. Vainsencher, B. Villalonga, T. White, Z. J. Yao, P. Yeh, A. Zalcman, H. Neven, and J. M. Martinis, Nature **574**, 505 (2019).

[7] Y. Wu, W.-S. Bao, S. Cao, F. Chen, M.-C. Chen, X. Chen, T.-H. Chung, H. Deng, Y. Du, D. Fan, M. Gong, C. Guo, C. Guo, S. Guo, L. Han, L. Hong, H.-L. Huang, Y.-H. Huo, L. Li, N. Li, S. Li, Y. Li, F. Liang, C. Lin, J. Lin, H. Qian, D. Qiao, H. Rong, H. Su, L. Sun, L. Wang, S. Wang, D. Wu, Y. Xu, K. Yan, W. Yang, Y. Yang, Y. Ye, J. Yin, C. Ying, J. Yu, C. Zha, C. Zhang, H. Zhang, K. Zhang, Y. Zhang, H. Zhao, Y. Zhao, L. Zhou, Q. Zhu, C.-Y. Lu, C.-Z. Peng, X. Zhu, and J.-W. Pan, Phys. Rev. Lett. **127**, 180501 (2021).

[8] H.-S. Zhong, H. Wang, Y.-H. Deng, M.-C. Chen, L.-C. Peng, Y.-H. Luo, J. Qin, D. Wu, X. Ding, Y. Hu, P. Hu, X.-Y. Yang, W.-J. Zhang, H. Li, Y. Li, X. Jiang, L. Gan, G. Yang, L. You, Z. Wang, L. Li, N.-L. Liu, C.-Y. Lu, and J.-W. Pan, Science **370**, 1460 (2020).

[9] H.-S. Zhong, Y.-H. Deng, J. Qin, H. Wang, M.-C. Chen, L.-C. Peng, Y.-H. Luo, D. Wu, S.-Q. Gong, H. Su, Y. Hu, P. Hu, X.-Y. Yang, W.-J. Zhang, H. Li, Y. Li, X. Jiang, L. Gan, G. Yang, L. You, Z. Wang, L. Li, N.-L. Liu, J. J. Renema, C.-Y. Lu, and J.-W. Pan, Phys. Rev. Lett. **127**, 180502 (2021).

[10] L. Bassham, A. Rukhin, J. Soto, J. Nechvatal, M. Smid, S. Leigh, M. Levenson, M. Vangel, N. Heckert, and D. Banks, A statistical test suite for random and pseudorandom number generators for cryptographic applications (2010).

[11] V. A. Marchenko and L. A. Pastur, Mat. Sb. (N.S.) **72**, 507 (1967).

[12] C. Villani, *Optimal Transport: Old and New*, Grundlehren der mathematischen Wissenschaften (Springer Berlin Heidelberg, 2008).

[13] S. Boixo, S. V. Isakov, V. N. Smelyanskiy, R. Babbush, N. Ding, Z. Jiang, M. J. Bremner, J. M. Martinis, and H. Neven, Nature Physics **14**, 595 (2018).

[14] X. Gao, M. Kalinowski, C.-N. Chou, M. D. Lukin, B. Barak, and S. Choi, Limitations of linear cross-entropy as a measure for quantum advantage (2021), arXiv:2112.01657 [quant-ph].

[15] M. Herrero-Collantes and J. C. Garcia-Escartin, Rev. Mod. Phys. **89**, 015004 (2017).

[16] J. M. Martinis *et al.*, Quantum supremacy using a programmable superconducting processor, dryad, dataset (2021).

[17] See Supplemental Material for the details of calculation.

[18] S. Oh and S. Kais, The Journal of Physical Chemistry Letters **13**, 7469 (2022).

[19] K. Tamura and Y. Shikano, in *International Symposium on Mathematics, Quantum Theory, and Cryptography*, edited by T. Takagi, M. Wakayama, K. Tanaka, N. Kunihiro, K. Kimoto, and Y. Ikematsu (Springer Singapore, Singapore, 2021) pp. 17–37.

[20] R. Flamary, N. Courty, A. Gramfort, M. Z. Alaya, A. Boisbunon, S. Chambon, L. Chapel, A. Corenflos, K. Fatras, N. Fournier, L. Gautheron, N. T. Gayraud, H. Janati, A. Rakotomamonjy, I. Redko, A. Rolet, A. Schutz, V. Seguy, D. J. Sutherland, R. Tavenard, A. Tong, and T. Vayer, Journal of Machine Learning Research **22**, 1 (2021).

[21] L. Laloux, P. Cizeau, J.-P. Bouchaud, and M. Potters, Phys. Rev. Lett. **83**, 1467 (1999).

[22] L. Laloux, P. Cizeau, M. Potters, and J.-P. Bouchaud, International Journal of Theoretical and Applied Finance **03**, 391 (2000).

[23] A. A. Lee, M. P. Brenner, and L. J. Colwell, Proceedings of the National Academy of Sciences **113**, 13564 (2016).

[24] J. Veraart, E. Fieremans, and D. S. Novikov, Magnetic Resonance in Medicine **76**, 1582 (2016), https://onlinelibrary.wiley.com/doi/pdf/10.1002/mrm.26059.

[25] L. Aparicio, M. Bordyuh, A. J. Blumberg, and R. Rabadan, Patterns **1**, 100035 (2020).

[26] J. Eisert, D. Hangleiter, N. Walk, I. Roth, D. Markham, R. Parekh, U. Chabaud, and E. Kashefi, Nature Reviews Physics **2**, 382 (2020).

[27] M. A. Nielsen and I. L. Chuang, *Quantum Computation and Quantum Information* (Cambridge University Press, Cambridge, England, 2010) p. 195.